



ELSEVIER

Catalysis Today 50 (1999) 629–636



Transition metals to sulfur binding energies relationship to catalytic activities in HDS: back to Sabatier with first principle calculations¹

Herve Toulhoat^{a,*}, Pascal Raybaud^a, Slavik Kasztelan^a, Georg Kresse^b, Jurgen Hafner^b

^aIFP, BP 311 92852, Rueil-Malmaison, France

^bITP-TU Wien, Wiedner Hauptstrasse 8-10, A-1040, Austria

Abstract

We have undertaken systematic calculations of transition metal sulfides bulk crystal structures, electronic and energetic properties at the first principles level (DFT, GGA, PW-USPP, PBC, implemented in the Vienna Ab initio Simulation Package, VASP). Relaxed cell parameters and ionic positions showed an excellent agreement with the experimental values. Computed and experimental cohesive energies agreed within 3%. We re-defined the metal–sulfur (M–S) bond strength as the cohesive energy per metal–sulfur bond: we show that all experimental HDS activities (Pecoraro and Chianelli, 1981) fit nicely on a single volcano master curve when plotted against this simple energetic parameter. Metallic (i.e. zero gap) ionic sulfides consistently exhibit the weakest M–S bonds and semi-conductor ionic-covalent sulfides the strongest. However, the Sabatier principle suggests a simple kinetic interpretation of this master curve. This new interpretation also accounts for the well known synergetic effects in mixed sulfides and therefore opens new prospects for exploratory applied research. © 1999 Elsevier Science B.V. All rights reserved.

Keywords: Transition metal sulfides; Sabatier principle; Synergetic effects; Density functional calculations

1. Introduction

Transition metal sulfides (TMS) encompass the only known class of stable catalytically active phases for the strongly sulfo-reductive hydroprocessing conditions. Currently, most hydroprocessing catalysts are mixed sulfides supported on transition alumina: Co(Ni)Mo(W)S. These systems are used because they present a so-called synergetic effect, i.e. the mixed sulfide is much more active than the individual mono-

metallic sulfides. The synergetic effect involving relatively low cost metals, these long ago empirically discovered mixed systems still present the best activity/cost ratio.

Although an enormous body of research has shed significant light on the subject over several decades [1], the origin of synergy, and more generally the rationale for TMS catalytic activity is still not understood. To gain more insight, we undertook ab initio calculations of energetic and electronic properties of ideal bulk TMS.

2. Former approaches

Pecoraro and Chianelli [2] were the first to report a systematic study of the intrinsic (per mole of metal at

*Corresponding author.

¹This work has been undertaken within the “GdR Dynamique Moléculaire Quantique Appliquée à la Catalyse”, a joint project of Centre National de la Recherche Scientifique, Technische Universität Wien, and Institut Français du Pétrole.

iso specific area) activity of bulk monometallic TMS in a model reaction, the hydrodesulfurization of dibenzothiophene at 400°C. Their results, establishing a relative activity scale for TMS as a function of the periodic position of the TM, were further roughly confirmed by several authors either for unsupported [3,4] or supported sulfides [5,6].

This activity scale spans nearly three orders of magnitude between the most active RuS_2 and the less active MnS . In their first interpretation of their activity results, Pecoraro and Chianelli [2] proposed that the latter could be organized along a single volcano curve if plotted against the TMS standard enthalpy of formation. By analogy with the Sabatier principle [7] they suggested that the optimum activity would correspond to an intermediate heat of adsorption of the organic sulfide reactant on the inorganic TMS surface which should correlate directly with the standard enthalpy of formation. This chemically intuitive theory remained however unconvincing, mainly because the less active MnS does present a mid-range standard enthalpy of formation, quite close to that of RuS_2 .

These early results triggered several attempts during the eighties and early nineties, to provide a theoretical foundation to the observed periodic trends in TMS activities, by means of various computational chemistry methods [8–12]. These studies tried to extract an activity index by combining parameters derived from the computed electronic structure data for the various models involved. None of these parameters proved definitively convincing both for their inability to predict qualitative essential features such as the correct location of the maximum activity, and for the crude limitations of the theoretical approach (e.g. unrelaxed clusters for modeling the surfaces of bulk sulfides), or too qualitative semi-empirical methods.

The work by Topsøe, Nørskov et al. [13,14], deserves a special mention as these authors tried to revisit the original concept of relating activity to metal–sulfur bond strength according to the Sabatier principle: they constructed an approximate theory to account for the influence of the d band filling through the transition series on the metal–sulfur bond strength of bulk TMS. The procedure is reported to fit with the predictions of first principle ASW-DFT-LDA calculations on model TMS of arbitrarily fixed CsCl structure.

This approximate metal–sulfur bond strength is shown to correlate with experimental activities in a monotonously decreasing way. As the maximum activity would accordingly correspond to the weakest metal–sulfur bond, these authors speculate that the limiting step in catalytic HDS would uniformly correspond to the energy of formation of a sulfur vacancy at the TMS surface, therefore removing any significance to the Sabatier principle in catalysis by TMS.

Their theory can be criticized however on several points: the weakness of the activity–bond strength correlation they report, the arbitrary omission of coordination and crystal structure in their theoretical representation of bulk TMS properties, and finally, the use of a definition of the metal–sulfur bond strength in a TMS, which does not reflect the cohesive energy content of the chemical bond itself. According to the related thermodynamic virtual process, their definition rather reflects the tendency to restore metal–metal bonds locally where an anionic vacancy has been created. Therefore, its periodic trends are largely dominated by the variation of the bulk modulus of the corresponding metal.

As catalysis by TMS is a surface process, the relevant bond strengths should be obviously the surface M–S bond strengths. Active sites for the various elementary steps involved in the HDS reaction are expected to correspond to coordinatively unsaturated surface M atoms (CUS), and the activation process to be related to the stabilization of transition states upon chemisorption at these CUS M atoms. Surface reconstruction is expected to be moderate for TMS relative to TM, in view of the former's stronger cohesion, and moreover, chemisorption induced de-reconstruction should occur in a way that M coordination spheres at the TMS surface will tend to reconstitute similarly as in the bulk. This was the intuition which led us, not unlike Chianelli et al., Topsøe et al. and others, to look for a correlation between bulk M–S bond strength and TMS catalytic activity. It is worth noting at this point that we have been addressing further the direct *ab initio* simulation of the relevant surface processes for the thiophene HDS on the MoS_2 (010) surfaces [31], [32], and the results were in a reasonable agreement with the conjecture above exposed. We distinguish ourselves from Topsøe et al. [13] point of view mainly from the fact that we think that as the reaction medium is strongly sulfo-reductive and therefore the TMS

being thermodynamically stable with respect to the TM, the cohesion in the TMS should be more relevant than the cohesion in the TM.

3. Definition of the metal–sulfur bond strength in TMS

It is worth recalling that there is no equivalence between the standard enthalpy of formation of a compound and its cohesive energy. The former is a concept of operational value for the experimental chemist: the thermodynamic path to the compound is referred to the elements in their *standard* state.

In the case of a TMS, the standard state of the transition element is the bulk solid metal, and the standard state of sulfur is also the solid state. The cohesive energy is a concept of the theoretical chemist, and it represents the energy of atomization of the compound. The energy of a bond is that fraction of the total cohesive energy of the compound which can be assigned to this particular bond.

This definition is basic and unambiguous. Another problem however, is to *locate* a bond between two atoms in a compound. The intuitive concept of bond founded modern chemistry, but paradoxically, its representation in the frame of quantum theory is still an active research topic [15,16]. In the case of a crystalline solid, the rigorous assignment of a bonding scheme is often quite a difficult task.

In a first approximation, however, shortest distance criteria can be applied for that purpose, once the atomic positions have been determined, on the ground that as a rule, the shorter the equilibrium distances between atoms the stronger the interactions.

For most transition metal sulfides comprising only one transition element, as is the case in the set studied by Pecoraro and Chianelli [2], the structures turn out to be simple enough so as to consider that they comprise only metal–sulfur strong bonds, so that the number n of such bonds per unit-cell is simply the number of cation per unit-cell time their coordination. In such simplest cases, the metal–sulfur bond strength is simply the cohesive energy per unit-cell divided by n .

Significant exceptions in the three TMS series are found in the pyrite structures RuS_2 , OsS_2 and IrS_2 [17] where the amount of cohesive energy associated to the

4 S_2 pairs per unit-cell, has to be evaluated and subtracted to the total cohesive energy per cell, leaving the total cohesive energy of metal–sulfur bonds. These remaining bonds are energetically equivalent and we are thus set back to the preceding case.

In a general way, once bonds have been located in a given inorganic structure by means of short distance criteria, the partition of the total cohesive energy between the energetically unequivalent bonds can always be evaluated computationally through the vacancy creation method applied in the present work: the total energy of relaxed supercells including anionic or cationic vacancies are computed and compared to that of the original perfect cell, the difference being assigned to the energy of all broken bonds. This virtual vacancy creation has to be repeated until the number of such balance equations matches the number of unequivalent bonds in the unit-cell.

4. Computational modeling methods

The methods implemented in VASP (Vienna Ab initio Simulation Package) [18–20] solve the time independent non-relativistic Schrödinger equation for the motion of electrons in the field of ions arranged in a periodic lattice. The solution is provided in the frame of the density functional theory (DFT) through a set of Kohn-Sham equations. The valence electrons interact with ionic cores through Vanderbilt ultrasoft non-local pseudopotentials, including scalar relativistic corrections [21].

The one electron pseudo-orbitals are expanded over a finite basis set of plane waves: the use of ultrasoft pseudopotentials allows a significant reduction in basis set size, which sets the main scaling order of the computational burden. Sets of k -points varying between $2 \times 2 \times 2$ and $10 \times 10 \times 10$ according to unit-cell sizes were used, determined according to the Blochl tetrahedron method.

The generalized gradient approximation (GGA) exchange and correlation functional was used for all SCF cycles involved in the full ionic relaxation. The latter was driven by the minimization of Hellmann–Feynmann forces. Atomic energies were evaluated for periodic models with non-interacting atoms located at the nodes of cubic grids of dimension 1 nm or more, and they included spin corrections.

For the TMS studied, the initial (experimental) asymmetric unit-cell was extracted from the inorganic crystal structures database (ICSD) [22]. The number n of M–S bonds per unit-cell was determined with the help of a 3D graphical representation of the unit-cell in real space, using the Solid_Builder module of MSI's software InsightII [23], which calculates connectivities through a ion–ion distance criterion.

Experimental cohesive energies (E_c exp. in Table 3) were calculated from tabulated [24] TMS standard enthalpies of formation and elements (M and S) standard enthalpies of sublimation, through the appropriate Born–Haber Cycle. Experimental M–S bond energies (E_b exp. in Table 3) were computed similarly to calculated M–S bond (E_b calc. in Table 3) energies by dividing experimental cohesive energies per unit-cells by n , after correction from *computed* energies of the S_2 pairs in the cases of pyrite structures (computed cohesive energies at the GGA level are referred to as E_c GGA in Table 3). Stable sulfides in usual hydroprocessing conditions of elements V, Cr, Mn, Fe, Co, Ni (3d series), Nb, Mo, Ru, Rh, Pd (4d series) and Ta, W, Re, Os, Ir, Pt (5d series) were considered throughout our study. All calculations

were performed on a Fujitsu VPP500 vector super-computer.

5. Results and discussion

All our results concerning TMS crystal structures are reported in Table 1, where the close correspondence between calculated and experimental data can be noticed. Also indicated in Table 1 are the numbers n of M–S bonds per stoichiometric unit.

These numbers characterize the p–d hybridization state of the M ions and hence the influence of the TMS structure on M–S bonds. As introduced in Section 3, they are the natural quantities which one should use for renormalizing cohesive energies in order to compare M–S bond strengths from one TMS to another.

As mentioned above the pyrite structures RuS_2 , OsS_2 and IrS_2 are well known for exhibiting S_2 pairs. Our calculations allowed us to evaluate the cohesive energy per S_2 pair at 1.44 eV (33.1 kcal/mol) in all cases: this figure multiplied by the number of S_2 pairs per unit-cell gave the amount of cohesive energy to

Table 1
Results of structure relaxations at the DFT/GGA level using VASP

TMS	f (eV)	d (Å)	$V_{\text{calc}}/V_{\text{exp}}$	System/SG no.	n
VS^a	0	0	0.95	Hexagonal/194	6
$Cr_2S_3^a$	0.033	0.0038	0.87	Trigonal/163	12
MnS^a	0	0	0.73	Cubic/225	6
FeS	0	0	0.85	Hexagonal/194	6
Co_9S_8	0.024	0.0032	0.98	Cubic/225	38
Ni_3S_2	0.020	0.0003	1.01	Trigonal/155	12
NbS_2	0.037	0.0065	1.01	Hexagonal/194	6
MoS_2	0.028	0.0045	1.03	Hexagonal/194	6
RuS_2	0.00025	0.0013	1.02	Cubic/205	6
Rh_2S_3	0.080	0.0054	1.03	Orthorhombic/60	12
PdS	0.045	0.0013	1.04	Tetragonal/84	4
TaS_2	0.046	0.0002	1.01	Hexagonal/194	6
WS_2	0.0068	0.0028	1.02	Hexagonal/194	6
ReS_2	0.090	0.015	1.08	Triclinic/1	6
OsS_2	0.00129	0.0019	1.02	Cubic/205	6
IrS_2	0.025	0	1.02	Cubic/205	6
PtS	0	0	1.06	Tetragonal/131	4

The experimental structures are taken as inputs. f and d correspond respectively to the maximum residual force and relative displacement from initial experimental crystallographic position observed for atoms in the unit-cell after complete relaxation. $V_{\text{calc}}/V_{\text{exp}}$ is the ratio of relaxed and initial unit-cell volumes. n is the number of M–S bonds per stoichiometric unit.

^a GGA spin-polarization should be required to account for magnetic ordering of these structures.

Table 2

Calculated electronic parameters (energies in eV) versus experimental specific activities

TMS	Valence electrons	Fermi level	DOS@Fermi	Band gap	Act. [2]
VS ^a	5	8.35	4.2	0	1.10
Cr ₂ S ₃ ^a	6	5.34	21.6	0	4.80
MnS ^a	7	4.48	12.7	0	0.60
FeS	8	7.90	5.27	0	1.10
Co ₉ S ₈	9	5.46	5.10	0	1.40
Ni ₃ S ₂	10	5.41	1.86	0	1.50
NbS ₂	5	4.42	8.5	0	1.70
MoS ₂	6	5.94	0.0	1.25	8.00
RuS ₂	8	7.38	0.0	0.56	379.50
Rh ₂ S ₃	9	6.84	0.0	0.19	106.10
PdS	10	4.41	0.5	0	12.50
TaS ₂	5	4.58	7.2	0	1.10
WS ₂	6	5.83	0.0	1.05	3.2
ReS ₂	7	5.15	0.0	1.16	39.40
OsS ₂	8	8.22	0.0	0.15	216.30
IrS ₂	9	8.32	11.0	0	171.80
PtS	10	5.3	0.0	0.06	16.00

^a GGA spin-polarization should be required to account for magnetic ordering of these structures.

subtract in order to assess correctly the M–S bond strength.

Table 2 compares HDS activities to the main electronic structure parameters resulting from our calculations. Clearly no direct correlation emerges from these comparisons except that sulfides of significant activ-

ities are ionic-covalent semi-conductors, and sulfides of low activities are rather ionic solids with a closed (computed) gap. The computed electronic structure of TMS is reported in a detailed way elsewhere [25].

Table 3 contains the experimental and calculated cohesive energies per mole, the M–S bond strengths

Table 3

Energetic parameters (in kcal/mol) versus experimental specific activities (*E_b* corresponds to the metal–sulfur bond strength defined as in text)

TMS	$-\Delta H^0_f$	<i>Ec</i> exp.	<i>Ec</i> GGA	<i>E_b</i> exp.	<i>E_b</i> calc.	Act. [2]	Act. [6]
RuS ₂	49.2	337.6	343.14	50.74	51.66	379.50	57.50
OsS ₂	35.3	359.05	365.28	54.34	55.38	216.30	60.90
IrS ₂	33.0	327.92	344.52	49.15	51.96	171.80	455.0
Rh ₂ S ₃	31.4	531.54	547.68	44.30	45.64	106.10	813.0
ReS ₂	42.7	361.82	377.73	60.30	62.95	39.40	34.30
PtS	19.5	222.76	225.07	55.69	56.27	16.00	15.50
PdS	16.9	175.26	179.41	43.81	44.85	12.50	20.14
MoS ₂	65.8	358.36	371.50	59.73	61.92	8.00	21.10
Cr ₂ S ₃ ^a	80.0	552.30	469.28	46.02	39.11	4.80	9.65
WS ₂	62.0	399.87	414.39	66.64	69.07	3.20	7.18
NbS ₂	84.8	392.95	396.41	65.49	66.07	1.70	3.54
Ni ₃ S ₂	17.2	495.80	498.10	41.32	41.51	1.50	3.49
Co ₉ S ₈	22.6	1658.27	1717.07	43.64	45.19	1.40	12.61
VS ^a	68.0	258.74	237.98	43.12	39.66	1.10	7.29
FeS	24.0	190.94	186.33	31.82	31.05	1.10	1.22
TaS ₂	84.6	404.71	417.16	67.45	69.53	1.10	2.24
MnS ^a	51.0	185.87	137.90	30.90	22.98	0.60	0.29

^a GGA spin-polarization should be required to account for magnetic ordering of these structures.

calculated according to the rule defined above from the experimental and calculated cohesive energies, the experimental standard heats of formation, and the experimental HDS activity per mole of metal as reported by Pecoraro and Chianelli [2]. One may prefer BET surface area normalized activities as a better indicator, however the BET area reported in [2] are rather low, at most $70 \text{ m}^2/\text{g}$, and therefore, come with a high uncertainty. Ledoux et al. [6] results obtained for highly dispersed TMS supported on C but at atmospheric total pressure and lower temperatures, show basically the same trends as those in [2] when expressed in TON units (h^{-1}), excepted that Rh and Ir are now more active than Ru and Os. The results in Table 3 have been sorted by decreasing catalytic activity (according to [2]), and it is evident from this that our results do not support the theory of Nørskov et al. [14], which predicts that activities should be inversely correlated to M–S bond strengths. Excepted for VS, Cr_2S_3 and MnS, for which spin-polarization effects should be included, experimental and calculated cohesive energies are in a very good agreement, with a linear

regression producing:

$$E_{\text{c GGA}} = 1.03 E_{\text{c exp}} + 0.04 \quad (R = 0.99). \quad (1)$$

Finally, experimental HDS activities are plotted in Fig. 1 against the M–S bond strengths calculated from the experimental cohesive energies. This simple plot presents the characteristic volcano shape, which we take, like others, but on a sounder basis, as indicative of a connection of catalysis by TMS with the Sabatier principle: indeed, solids with the extremes of M–S bond strengths are practically inactive, while those with intermediate M–S bond strengths are active. The same kind of volcano plot is obtained if now the atmospheric pressure data of [6] are plotted in ordinates, excepted that the maximum is now shifted to Rh_2S_3 , and IrS_2 is now above RuS_2 and OsS_2 on the right-hand side of the plot.

The solid curve in Fig. 1 is a theoretical fit of a kinetic equation previously proposed [26], assuming a heterolytic mechanism as the common limiting step of HDS on TMS. Here, the model assumes a linear relationship between the standard enthalpies of adsorption of the sulfur compounds participating in

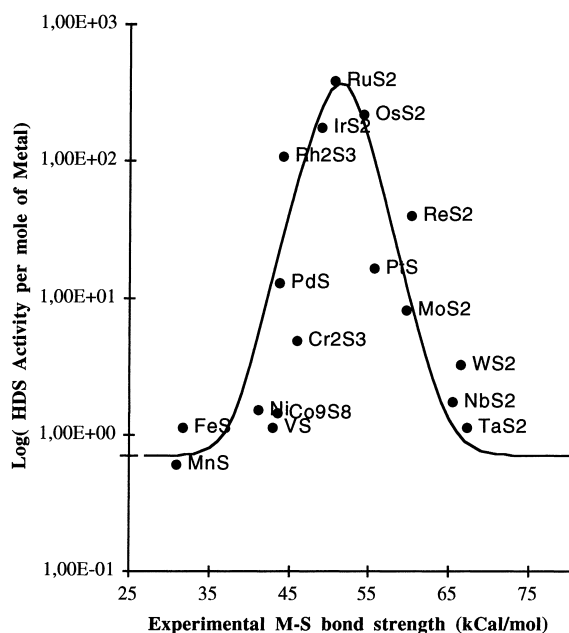


Fig. 1. Experimental specific activities in DBT HDS [2] versus M–S bond strengths of transition metal sulfides (black dots). The solid line is a fit of a kinetic model assuming a heterolytic mechanism for HDS [26,27].

the limiting step, and the M–S bond strength. Interestingly, the model does predict a temperature and pressure dependant abscissa for the maximum activity, and indeed Rh_2S_3 is expected to be the more active at atmospheric pressure. This interpretation will be detailed elsewhere [27].

An important pre-requisite for any theory of catalysis by TMS is to provide an explanation for the spectacular synergetic effects existing in the Co(Ni)–Mo(W)S bulk or supported systems. It can be seen in Fig. 1 that 3d TMS where M is Ni, Co or Fe are on the low bond strength side of our plot, while MoS_2 and WS_2 are on the high bond strength side.

It is well established [28–30] that in the synergetic systems one has to deal with mixed sulfides, where the 3d ions “decorate” coordinatively unsaturated “edges” of the lamellar sulfides of Mo or W. Hence, although no precise local structure for the decorating sites has been demonstrated to date, it is quite likely that the two metals share sulfur anions, which would then be characterized by a M–S bond strength intermediate between those of the two parent TMS.

Indeed, if one takes the arithmetic mean for the relevant bond strength in mixed synergetic sulfides, our volcano plot predicts a catalytic activity close to the optimum, i.e. in the range of that exhibited by RuS_2 or OsS_2 . The predicted order in HDS activity for the mixed systems is indeed the experimental one (under pressure in the range 30–100 bar), namely: $\text{CoMoS} \{373\} \approx \text{RuS}_2 \{379\} > \text{NiMoS} \{365\} > \text{NiWS} \{211\} > \text{CoWS} \{129\} \gg \text{FeMoS} \{53\}$. Where bracketed figures are the specific activities per mole of promoter metal, computed according to our kinetic model.

6. Conclusions

A simple and consistent re-definition of the metal–sulfur bond strength in transition metal sulfides opens new theoretical and practical perspectives to research on hydrotreating catalysts. This energetic parameter allows experimental TMS activities to be clearly organized into a volcano plot, suggesting a unifying interpretation based on the Sabatier principle. It is suggested that this behavior is kinetically determined, with the most active TMS depending on reaction

conditions. First principles calculations of TMS electronic and structural properties show on the one hand that this parameter can be precisely computed ab initio for any hypothetical structure, and on the other hand that there is no direct relationship between catalytic activity and the DOS characteristics. These findings then allow us to propose a new explanation for the origin of the promotion effects in mixed sulfides of Co(Ni)+Mo(W).

References

- [1] H. Topsøe, B.S. Clausen, F. Massoth, *Hydrotreating Catalysis in Catalysis, Science and Technology*, vol.11, Springer, Berlin, 1996.
- [2] T.A. Pecoraro, R.R. Chianelli, *J. Catal.* 67 (1981) 430.
- [3] M. Lacroix, N. Boutarfa, C. Guillard, M. Vrinat, M. Breyse, *J. Catal.* 120 (1989) 473.
- [4] M. Lacroix, H. Marrakchi, C. Calais, M. Breyse, C. Forquy, *Stud. Surf. Sci. Catal.* 59 (1991) 277.
- [5] J.P.R. Vissers, C.K. Groot, E.M. van Oers, V.H.J. de Beer, R. Prins, *Bull. Soc. Chim. Belg.* 93 (1984) 813.
- [6] M.J. Ledoux, O. Michaux, J. Agostini, P. Panissod, *J. Catal.* 102 (1986) 275.
- [7] P. Sabatier, *Berichte der Deutschen Chem. Gesellschaft* 44 (1911) 1984.
- [8] S. Harris, R. Chianelli, *J. Catal.* 86 (1984) 400.
- [9] S. Harris, R. Chianelli, *J. Catal.* 98 (1986) 17.
- [10] J.K. Burdett, J.T. Chung, *Surf. Sci. Lett.* 236 (1990) L353.
- [11] T.S. Smit, K.H. Johnson, *Catal. Lett.* 28 (1994) 361.
- [12] T.S. Smit, K.H. Johnson, *J. Mol. Cat.* 91 (1994) 207.
- [13] H. Topsøe, B.S. Clausen, N.Y. Topsøe, J. Hyldtoft, J.K. Nørskov, *ACS, Petrol. Div. Prepr.* 38 (1993) 638.
- [14] J.K. Nørskov, B.S. Clausen, H. Topsøe, *Catal. Lett.* 13 (1992) 1.
- [15] R.F.W. Bader, *Atoms in Molecules*, Oxford Science Publications, 1990.
- [16] B. Silvi, A. Savin, *Nature* 371 (1994) 683.
- [17] P. Raybaud, G. Kresse, J. Hafner, H. Toulhoat, *J. Phys.: Condens. Matter* 9 (1997) 11085.
- [18] G. Kresse, J. Hafner, *Phys. Rev. B* 47 (1993) 558.
- [19] J. Furthmüller, J. Hafner, G. Kresse, *Phys. Rev. B* 50 (1994) 15606.
- [20] <http://tph.tuwien.ac.at/~vasp> and references therein.
- [21] D. Vanderbilt, *Phys. Rev. B* 41 (1990) 7892.
- [22] ICSD, Release 95/2, Fachinformationszentrum Karlsruhe, 1995.
- [23] Insight[®] II, a software program from MSI of San Diego, 9685 Scranton Road, CA 92121-3752, USA.
- [24] *Handbook of Physics and Chemistry*, 76th ed., CRC Press, Boca Raton, 1995.
- [25] P. Raybaud, G. Kresse, J. Hafner, H. Toulhoat, *J. Phys.: Condens. Matter* 9 (1997) 11107.

- [26] S. Kasztelan, in: *Hydrotreating Technology for pollution Control, Catalysts, Catalysis and Process*, Chemical Industries, vol. 67, Marcel Dekker, New York, 1996, p. 29.
- [27] H. Toulhoat, P. Raybaud, S. Kasztelan, G. Kresse, in preparation.
- [28] N.Y. Topsøe, H. Topsøe, *J. Catal.* 84 (1983) 386.
- [29] S. Kasztelan, H. Toulhoat, J. Grimblot, J.P. Bonnelle, *Appl. Catal.* 13 (1984) 127.
- [30] J.M. Tonnerre, D. Raoux, J.C. De Lima, H. Toulhoat, D. Espinat, *J. de Physique* 12 48 (1987) C9–1137.
- [31] P. Raybaud, G. Kresse, J. Hafner, H. Toulhoat, *Phys. Rev. Lett.* 80 (1998) 1481.
- [32] P. Raybaud, G. Kresse, J. Hafner, H. Toulhoat, *Surf. Sci.* 407 (1998) 237.